Fig. 3. Ferroelectric hysteresis loops of $(NH_4)_3H$ $(SO_4)_2$. (a) in Phase VII ($p=5.6$ kbar, $T=-86.6\,°C$), (b) in Phase VI ($p=5.6$ kbar, $T=-56.5\,°C$). Frequency: 50 Hz.

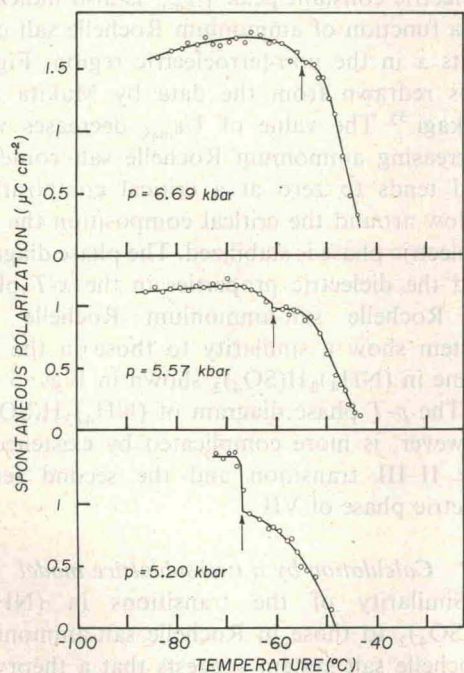
Fig. 4. Temperature dependence of the spontaneous polarization of $(NH_4)_3H(SO_4)_2$ at different pressures. On heating process. The vertical arrows indicate the VII–VI transition.

the vertical arrows in Fig. 4. The discontinuity becomes unclear with increasing pressure; this is consistent with the diminution in the thermal hysteresis of transition.
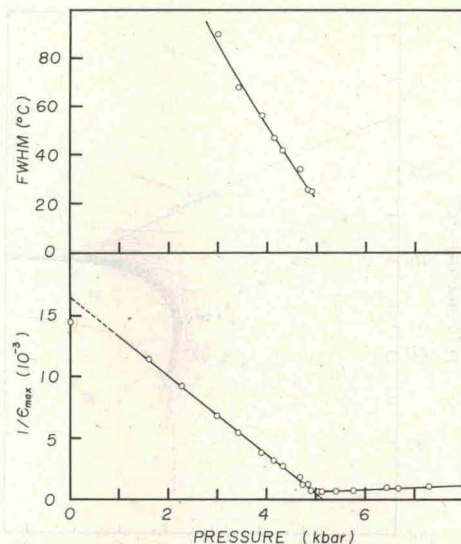

Fig. 5. Hydrostatic pressure dependence of the full width at half maximum (FWHM) of the broad peak of dielectric constant (above) and the inverse of the maximum value of dielectric constant (below) along the c^*-direction of $(NH_4)_3H(SO_4)_2$. In the below figure the inverse of the dielectric constant at the upper Curie point is plotted for the pressure region above 5 kbar.

Figure 5 shows the pressure dependence of the inverse of the maximum dielectric constant and of the full width at half maximum (FWHM) of the broad dielectric constant peak. Above about 1 kbar, the inverse of the maximum dielectric constant $1/\varepsilon_{max}$ linearly decreases with increasing pressure as $1/\varepsilon_{max} = C^*(p_0 - p)$. The parameters are determined as $C^* = (3.20 \pm 0.03) \times 10^{-3}$ kbar^{-1} and $p_0 = 5.1 \pm 0.1$ kbar. The ferroelectric VI Phase is stabilized above 5.0 kbar; slightly below the critical pressure p_0. In Fig. 5, above 5 kbar the inverse of the maximum dielectric constant at the upper Curie point (the III–VI or II–VI transition point) is plotted. The value of $1/\varepsilon_{max}$ slightly increases with increasing pressure in this pressure region. The full width at half maximum (FWHM) of the broad dielectric constant peak which is more than $100\,°C$ at 0 kbar rapidly decreases with increasing pressure as seen in Fig. 5.

Figure 6 indicates the pressure-temperature phase diagram below room temperature. In the figure the solid circles indicate the peak positions of the dielectric constant observed in constant pressure measurements. Contour lines of equal dielectric constant are indicated by
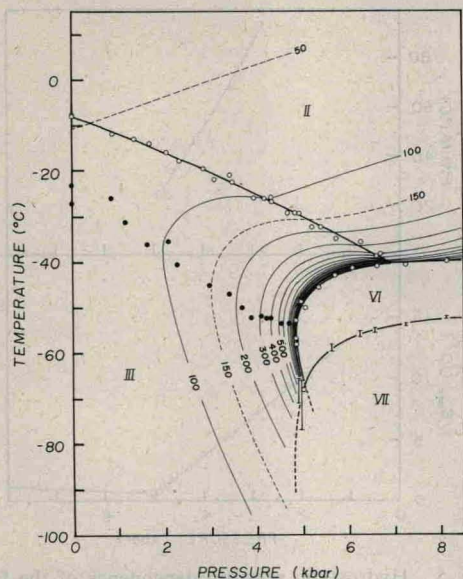
Fig. 6. Pressure-temperature phase diagram of
$(NH_4)_3H(SO_4)_2$ below room temperature. Open
circles and vertical short bars indicate observed
transition points. Solid circles indicate the maximum
positions of the broad peak of the dielectric constant
along the c^*-direction at $p=$constant measurements.
Contour lines of equal dielectric constant are shown
in Phases II and III.

thin curves for the non-ferroelectric phases of
II and III. It is noted that a ridge of the di-
electric constant extends in a direction roughly
parallel to the II–III phase boundary. It is
evident that the solid circles should be on the
trajectory of contact points of contour curves
and $p=$constant lines.

§4. Discussion

4.1 Comparison with the Rochelle salt-am-
monium Rochelle salt system

The results shown in Fig. 6 indicate that the
polarization fluctuation which brings about the
high pressure VI Phase is described in the two
dimensional pressure-temperature space. Simi-
lar situation was already reported for Rochelle
salt-ammonium Rochelle salt system by Makita
and Takagi:[5] As the contents of ammonium
Rochelle salt decrease from about 15 at. % a
broad peak of dielectric constant becomes more
and more conspicuous, and below about 2.5
at. % of ammonium Rochelle salt contents the
peak of dielectric constant splits into double
maxima stabilizing a ferroelectric phase be-
tween them.

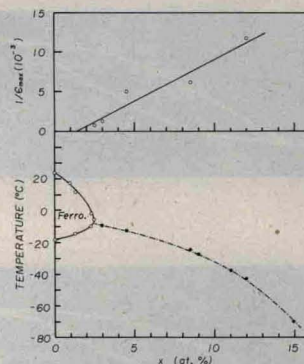Figure 7 shows the phase diagram of Rochelle

Fig. 7. Phase diagram of the Rochelle salt-
ammonium Rochelle salt system (below) and the
ammonium Rochelle salt content x dependence of
the inverse of the maximum dielectric constant
(above). In the below figure the position of the
maximum dielectric constant in the non-ferroelectric
phase is indicated by solid circles.

salt- ammonium Rochelle salt system. The
inverse of the maximum value at the broad
dielectric constant peak $1/\varepsilon_{max}$ is also indicated
as a function of ammonium Rochelle salt con-
tents x in the non-ferroelectric region. Figure
7 is redrawn from the data by Makita and
Takagi.[5] The value of $1/\varepsilon_{max}$ decreases with
decreasing ammonium Rochelle salt contents,
and tends to zero at a critical composition.
Below around the critical composition the fer-
roelectric phase is stabilized. The phase diagram
and the dielectric properties in the x-T plane
of Rochelle salt-ammonium Rochelle salt
system show a similarity to those in the p-T
plane in $(NH_4)_3H(SO_4)_2$ shown in Figs. 5 and
6. The p-T phase diagram of $(NH_4)_3H(SO_4)_2$,
however, is more complicated by existence of
the II–III transition and the second ferro-
electric phase of VII.

4.2 Calculation by a two-sublattice model

Similarity of the transitions in $(NH_4)_3$
$H(SO_4)_2$ to those in Rochelle salt-ammonium
Rochelle salt system suggests that a theory of
Rochelle salt-type ferroelectrics may also be
applied to $(NH_4)_3H(SO_4)_2$. In this section,
Mitsui's two-sublattice model of Rochelle
salt[4] is modified to apply to a free crystal and
is tried to apply to the problem of the phase
transitions in $(NH_4)_3H(SO_4)_2$. Recent struc-
tural analysis showed that the non-ferro-
electric II Phase allows an antiferroelectric
arrangement of dipoles. Also a long-period